

Wave overtopping and splash-up at seawalls with bullnose

Le Hai Trung^{*}, Dang Thi Linh, Tang Xuan Tho, Nguyen Truong Duy, Tran Thanh Tung

Thuyloi University, Hanoi, Vietnam

*E-mail: trung.l.h@tlu.edu.vn/haitrungle81@gmail.com

Received: 14 May 2020; Accepted: 16 July 2020

©2020 Vietnam Academy of Science and Technology (VAST)

Abstract

Seawalls have been erected to protect hundreds of towns and tourism areas stretching along the coast of Vietnam. During storm surges or high tides, wave overtopping and splash-up would often threaten the safety of infrastructures, traffic and residents on the narrow land behind. Therefore, this study investigates these wave-wall interactions via hydraulic small scale model tests at Thuyloi University. Remarkably, the structure models were shaped to have different seaward faces and bullnoses. The wave overtopping discharge and splash run-up height at seawalls with bullnose are significantly smaller than those without bullnose. Furthermore, the magnitude of these decreasing effects is quantitatively estimated.

Keywords: Bullnose, overtopping, physical model, seawall, splash-up, wave flume.

INTRODUCTION

Historically, seawalls have been built along the coastlines to protect the land from erosion and flooding and sometimes provide additional amenity value. Typically, structures are either massive vertical retaining walls or very steep face ones. For example, Chinese people constructed a steep stone seawall running along Hangzhou bay several centuries ago. The structure had served to protect people and their property under many recorded hazards from sea and river [1].

In severe weather conditions, big waves would attack and generate significant overtopping and splashing up. Wave overtopping at seawall has been intensively investigated in many works including physical models [2, 3], numerical simulations [4] and even in situ tests and field measurements [5]. To reduce wave overtopping, the design would often consist of a seaward overhang in forms of recurve, parapet, return wall, bullnose. Notably, Pearson et al., (2005) [6] investigated the recurve/parapet which gives significant reductions of wave overtopping. Based on research, knowledge has been gradually accumulated thus leading to proper and economical design of seawalls as published in a large number of handbooks and guidelines [7–9].

Along the coast of Vietnam, seawalls have become more and more popular and reliable to protect an increasing number of towns and tourism hotspots, especially since 2000s. In fact, seawalls would be newly constructed or upgraded from existing protection structures. In the latter case, concrete blocks of various shapes are built or placed on the crest of a revetment/dike. By doing so, the crest is leveled up significantly while the landscape is not violently affected. However, the practice of design is very much dependent on experience with dikes and revetments, which has been long applied in Vietnam.

Therefore, the paper aims to determine the performance of seawall blocks on a steep revetment, focusing on wave overtopping and splashing up. To this end, physical experiments were conducted on three different cross-sections of seawall in a wave flume.

Remarkably, the models are tested with and without bullnose. Section 2 describes the setup of the experiments including wave flume, cross-sections of the structure tested, wave conditions, measurement devices and test scenarios. Section 3 presents the test results and discusses how effectively the bullnoses prevent and reduce wave overtopping as well as splashing up.

METHODOLOGY

Holland wave flume

All experiments were carried out in the Holland wave flume at the Integrated Hydraulic Laboratory at Thuyloi University. The flume measures 45 m long (effective), 1.0 m wide and 1.2 m high. The wave maker is equipped with an advanced automated system of active reflection compensation (ARC) and may generate irregular waves with height of up to 30 cm and a peak period of 3.0 seconds. Measurement devices were manufactured and installed by HR Wallingford.

The model structures and wave parameters are selected according to a length scale of 1/15, a scale ratio [10] of 15. A foreland made of fine sand is shaped with an inclination of 1/50. The seawall is positioned on the top of a steep base (cot $\alpha = 1.5$). Figure 1 sketches the experiment configuration and the arrangement of all measurement devices.

Measurement devices

We used capacitance-type wave gauges to record wave signals at sampling frequency of up to 100 Hz. Four gauges were used to separate reflected waves and thus determine incident waves at the front of the structures. The distances between these gauges are carefully selected so that singularities in the wave separation can be properly avoided. Two other gauges are utilised to determine waves in front of the board (deep water) and at the middle of the foreland, respectively (fig. 1).

A tank was placed right behind the wall to collect all water produced by overtopping wave and splashing up. A pumping system was set up to keep transferring the water to a bucket for measuring the volume. Besides, a digital camcorder is deserved to capture the splashing-up height with regard to a vertical ruler on side

of the flume. Additionally, we used another camcorder to record the overview of every experiment.

In short, three groups of parameters were measured including wave characteristics, overtopping volumes and splash run-up height.

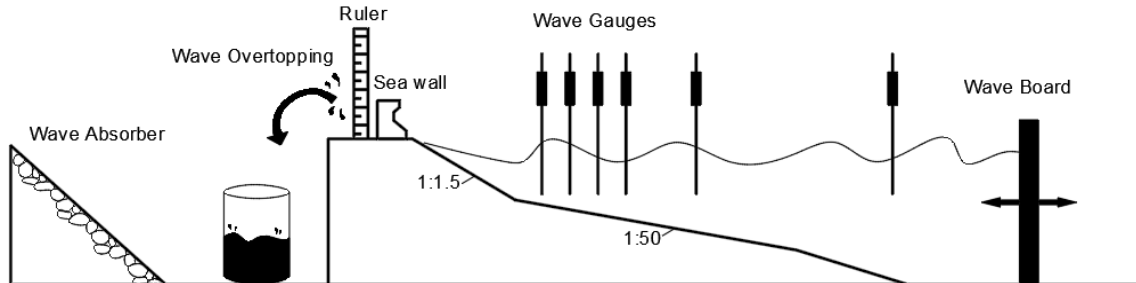


Figure 1. Experimental setup in the wave flume including a wave board, a foreland, a base, a seawall, an overtopping water tank and a wave absorber (not to scale)

Cross-sections of the seawall model

The cross-section of any structure plays a vital role in the wave-structure interaction, especially overtopping and splashing up. Therefore, we investigated the performance of

different seaward faces including curved (fig. 2a), steep (fig. 2b) and straight (fig. 2c). In general, the studied structural configurations would be found similar to coastal structures of complex geometries as described in Zanuttigh (2016) [11].

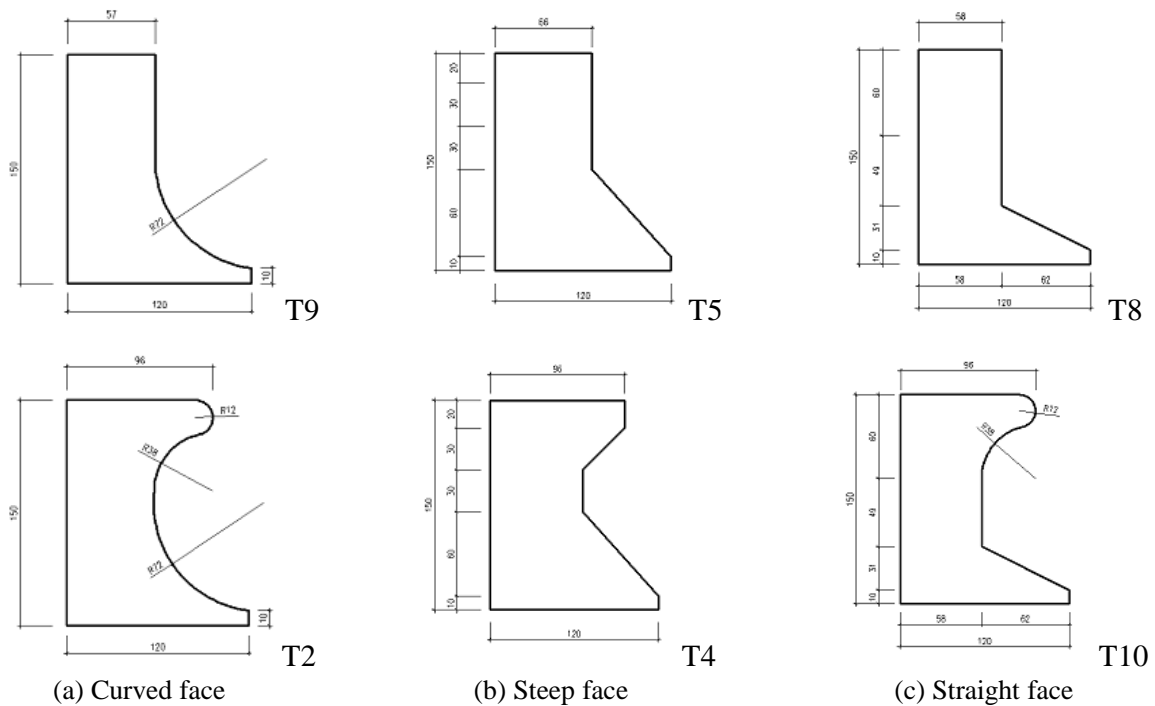


Figure 2. Different cross-sections of seawall with and without bullnose

Each type of wall was shaped with and without bullnose, e.g. T2 is curved one with bullnose and T9 without bullnose. Remarkably, the bullnose is relatively large with regard to

the dimension of the entire wall. These seawall models are made of mica plastic. They are all 150 mm high, 120 mm and 96 mm wide at toe and crest, respectively.

Test scenarios

We conducted a series of experiments under two wave conditions which have standard JONSWAP spectrum. In which, the wave heights were 0.15, 0.17 m while wave periods were 1.5 s and 1.6 s, respectively (table 1). Each wave condition was generated in the flume filled with two depths of 0.50 m and 0.55 m in order to assess the influence of water level (especially low tide and high tide) on wave overtopping and splashing up. Every test consists of at least 500 waves in order to reproduce the entire spectra and to generate wave overtopping with stable discharges.

Table 1. Wave conditions in the wave flume

d [m]	H_{m0} [m]	T_p [s]
0.50	0.15	1.5
0.50	0.17	1.6
0.55	0.15	1.5
0.55	0.17	1.6

For every cross-section, all tests were carried out twice to check the consistency of

the measured results. A test name consists of four parts including water depth d , wave height H , wave period T , and its order (the 1st test is denoted as ‘i’ and ‘ii’ for the 2nd one). In practice, several tests were repeated three or four times in case of suspecting the results.

RESULTS AND DISCUSSION

Wave overtopping discharge

We directly measured the total wave overtopping volume V [m³] and test duration t [second]. As the wave flume is 1 m wide, the averaged unit overtopping discharge q [m³/s per m] is therefore simply derived from these two parameters:

$$q = \frac{V}{t} \tag{1}$$

Tables 2–4 provide all values of V , t and q for curved seawall models (T2 and T9), steep ones (T4 and T5), and straight ones (T10 and T8). Due to the small amount of overtopping taking place, discharge q is expressed with a constant of 10^{-3} .

Table 2. Wave overtopping discharge on curved seawalls

Scenarios	T2			T9			$k_{bn}(q_{T2}/q_{T9})$
	V [m ³]	t [s]	$q_{T2} 10^{-3}$ [m ³ /s/m]	V [m ³]	t [s]	$q_{T9} 10^{-3}$ [m ³ /s/m]	
d50H15T15 i	0.003	750	0.004	0.030	750	0.040	0.100
d50H15T15 ii	0.004	750	0.005	0.035	750	0.047	0.107
d50H17T16 i	0.010	800	0.013	0.045	800	0.056	0.231
d50H17T16 ii	0.011	800	0.014	0.042	800	0.053	0.267
d55H15T15 i	0.060	750	0.08	0.410	800	0.513	0.156
d55H15T15 ii	0.060	750	0.08	0.420	800	0.525	0.152
d55H17T16 i	0.105	800	0.131	0.265	750	0.353	0.371
d55H17T16 ii	0.110	800	0.138	0.260	750	0.347	0.398

Table 3. Wave overtopping discharge on steep seawalls

Scenarios	T4			T5			$k_{bn}(q_{T4}/q_{T5})$
	V [m ³]	t [s]	$q_{T4} 10^{-3}$ [m ³ /s/m]	V [m ³]	t [s]	$q_{T5} 10^{-3}$ [m ³ /s/m]	
d50H15T15 i	0.062	750	0.083	0.065	750	0.087	0.958
d50H15T15 ii	0.065	750	0.087	0.070	750	0.093	0.932
d50H17T16 i	0.002	800	0.003	0.100	800	0.125	0.024
d50H17T16 ii	0.002	800	0.002	0.110	800	0.138	0.015
d55H17T16 i	0.135	800	0.169	0.495	800	0.619	0.273
d55H17T16 ii	0.125	800	0.156	0.485	800	0.606	0.257

Table 4. Wave overtopping discharge on straight seawalls

Scenarios	T10			T8			$k_{bn} (q_{T10}/q_{T8})$
	$V [m^3]$	$t [s]$	$q_{T10} 10^{-3} [m^3/s/m]$	$V [m^3]$	$t [s]$	$q_{T8} 10^{-3} [m^3/s/m]$	
d50H15T15 i	0.004	750	0.005	0.032	750	0.043	0.117
d50H15T15 ii	0.003	750	0.004	0.035	750	0.047	0.086
d50H17T16 i	0.009	800	0.011	0.075	800	0.094	0.117
d50H17T16 ii	0.010	800	0.013	0.072	800	0.090	0.144
d55H15T15 i	0.045	750	0.060	0.280	750	0.373	0.161
d55H15T15 ii	0.050	750	0.067	0.285	750	0.380	0.176
d55H17T16 i	0.110	750	0.147	0.330	800	0.413	0.356
d55H17T16 ii	0.105	750	0.140	0.340	800	0.425	0.329

From the measured values above, we plot the dimensionless crest freeboard R_c/H_{m0} against dimensionless discharge $q/\sqrt{gH_{m0}^3}$ in fig. 3, fig. 4 and fig. 5. It is clear that the higher the freeboard, the smaller the discharge

despite having a bullnose or not. In general, steep face models (T5 and T4) would produce the highest overtopping discharge while straight ones generate the lowest overtopping rate (T8 and T10).

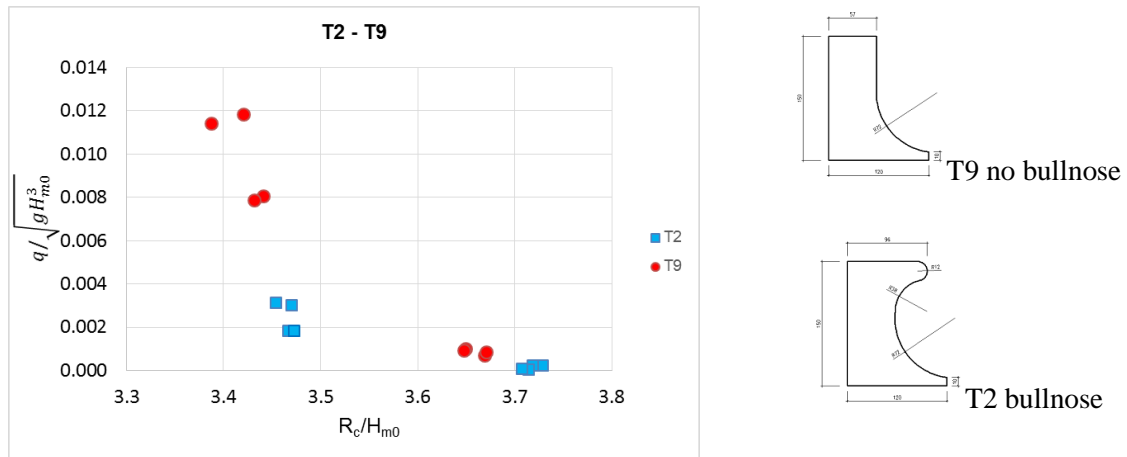


Figure 3. Dimensionless discharge vs. crest freeboard, curved face models T2 and T9

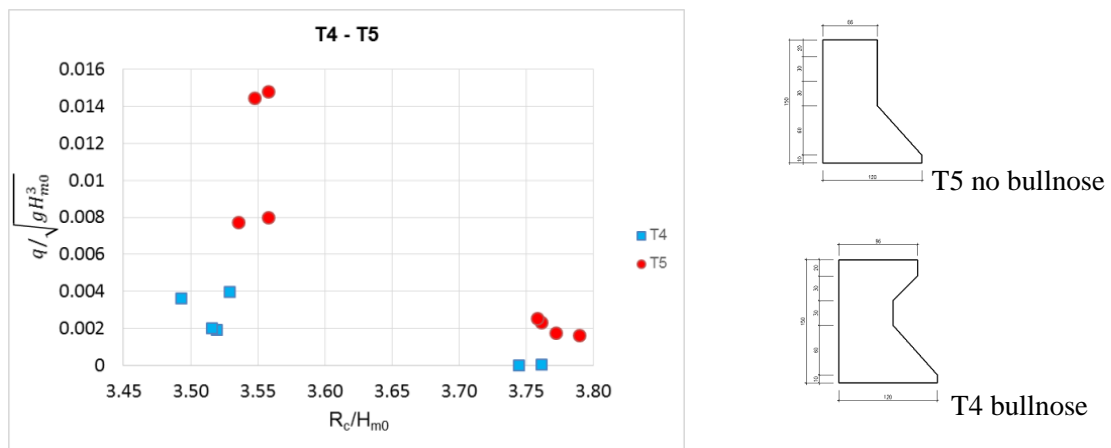


Figure 4. Dimensionless discharge vs. crest freeboard, steep face models T4 and T5

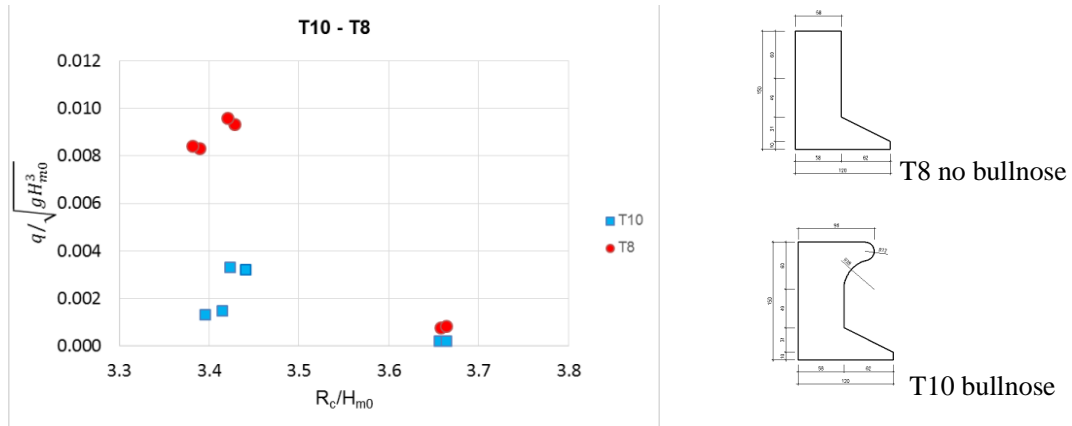


Figure 5. Dimensionless discharge vs. cress freeboard, straight face models T10 and T8

Having no bullnose, overtopping discharges are similar between models T9 and T8, and slightly less than on T5. It would be due to the steep face that stimulates water run-up to reach higher than in cases of straight and curved ones. Maximum value of $q/\sqrt{gH_{m0}^3}$ is up to about 0.015 for T5 while that is 0.012 and 0.01 for T9 and T8, respectively.

Interestingly, bullnose shows the most significant effect on steep face models when $q/\sqrt{gH_{m0}^3}$ drops from (0.008 ~ 0.014) for T5 to (0.002 ~ 0.004) for T4. In the mean while, overtopping rates reduce from (0.008 ~ 0.012) for T9 to (0.002 ~ 0.003) for T12 and $q/\sqrt{gH_{m0}^3}$ is (0.008 ~ 0.01) and (0.001 ~ 0.003) on T8 and T10, respectively. And for rather high freeboard, there would be hardly any water overtopping the curved seawall T2.

Reduction factor due to bullnose effect

It is the bullnose that considerably reduces the overtopping discharge on all seawall models tested. Based on EurOtop 2006 [12], Bruce et al. (2010) [13] described the mean overtopping rates for various configurations of vertical and composite structures. Inspired by these existing theories, a discharge reduction factor is proposed to quantitatively estimate the effect of bullnose as follows:

$$k_{bn} = \frac{q_{bn}}{q_{nobn}} \quad (2)$$

In which: q_{bn} and q_{nobn} are overtopping rates on seawall model with and without bullnose, respectively. The smaller the factor, the greater the amount of discharge which is decreased due to the bullnose.

In tables 2–4 above, overtopping rates without bullnoses q_{nobn} are assigned to q_{T9} , q_{T5} and q_{T8} while those with bullnoses q_{bn} correspond to q_{T92} , q_{T4} and q_{T10} . And the calculated values of k_{bn} vary over a comparable range for curved (0.1 ~ 0.398) and straight (0.085 ~ 0.356) seawalls. Not surprisingly, the steep face model has the most scattering k_{bn} which fluctuates from 0.014 to 0.954. For comparison, Pearson et al., (2005) [6] paid attention to seawalls with high freeboard and under wave breaking conditions. In their study, recurve/parapet shows significant effect with reduction factor larger than 0.95.

Three sections all have the smallest k_{bn} with water depth of 0.50 m in the wave flume; and curved and straight ones get the maximum value of the factor with 0.55 m water depth (table 5). Therefore, it seems that bullnose may cause more clear effects with lower water level rather than higher one. For curved and straight seawalls, higher waves lead to greater k_{bn} , i.e. the influence of bullnose becomes less significant. In contrast, bullnose of steep wall is more effective in decreasing overtopping discharge when wave gets higher.

Kortenhaus et al., (2004) [14] first discussed systematically a huge volume of data on overtopping at seawalls with recurves/wave

return walls/parapets. The authors did introduce a simple reduction factor depending on geometrical dimensions of the parapets. Indeed, a larger number of measurements are highly

recommended in order to establish the relationship between k_{bn} and the configuration of the seawall as well as the bullnose shape in the coming steps of the present study.

Table 5. Comparison of k_{bn} among different seaward faces

k_{bn}	Curved	Steep	Straight
Max	0.398 d55H17T16ii	0.954 d50H15T15i	0.356 d55H17T16i
Min	0.1 d50H15T15i	0.014 d50H17T16ii	0.085 d50H15T15ii
Averaged	0.222	0.410	0.186

Run-up height of water splash

The wave-structure interaction of seawall is often more intensive and spectacular than those of dikes and revetments. It is the manner of water splashing up that may increase the danger to men, properties and vehicles behind a wall. However, few works have been conducted to quantitatively determine the splash-up [15]. The present study aims to ascertain how bullnose affects the splash run-up height on various shapes of seawalls.

We counted the number of times that a water splash exceeds a certain height h_{sp} that is marked on the vertical ruler attached to the flume (fig. 1). For a clear recognition, the minimum height is set at 0.3 m from the structure base, noted that all seawall models are 0.15 m high. Besides, measurements give a maximum run-up height of 1.3 m in the entire data set.

Processing the recorded data, we propose an exceedance probability of a certain run-up level as follows:

$$P_{sp} = \frac{n_{\overline{h_{sp}}}}{N_{sp}} \tag{3}$$

With: $n_{\overline{h_{sp}}}$ the number of waves that splash over a given run-up level $\overline{h_{sp}}$ and N_{sp} the total number of waves splashing up over the minimum level of 0.3 m in each experiment. Using this new parameter, we calculate P_{sp} with corresponding dimensionless run-up level h_{sp}/H_{m0} . The obtained results are then plotted in figs. 6–8 for three pairs of seawall models (with and without bullnose).

Obviously, the chance that a wave splash reaches a high run-up level is less than that of a low level. On one hand, data show large spreading for seawalls without bullnose. It means there are many splashes with either low or high run-up heights.

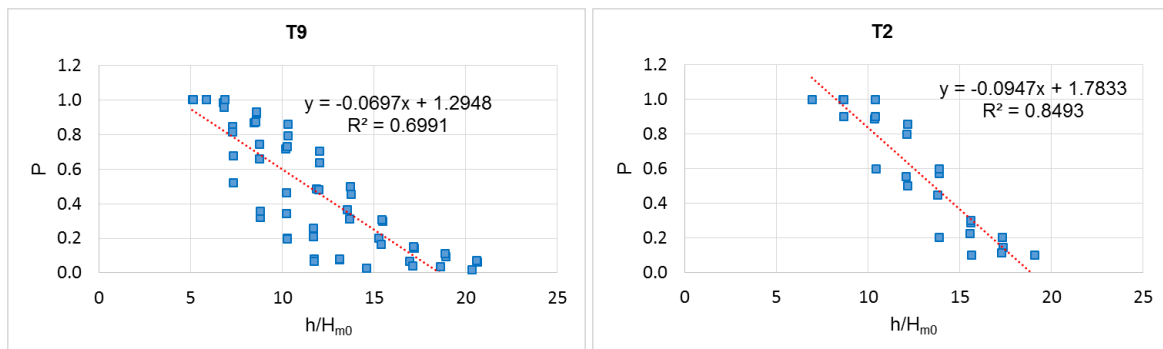


Figure 6. Exceedance probability of splash run-up height on curved face model T9 (no bullnose) and T2 (bullnose)

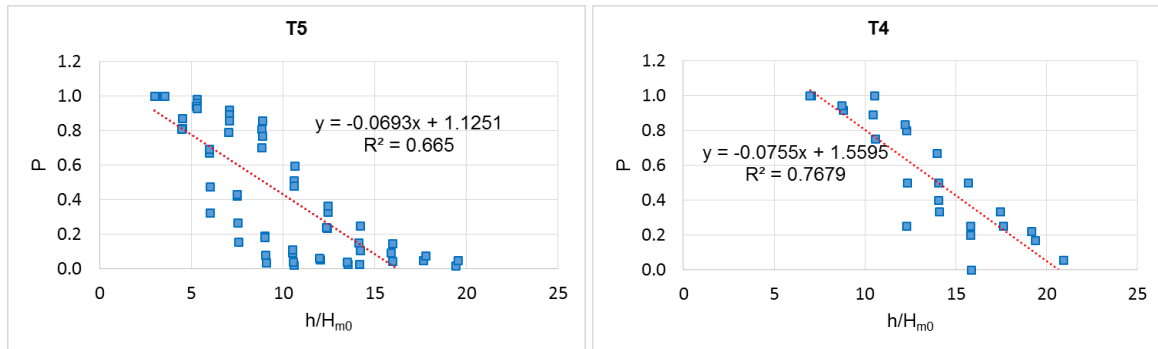


Figure 7. Exceedance probability of splash run-up height on steep face model T5 (no bullnose) and T4 (bullnose)

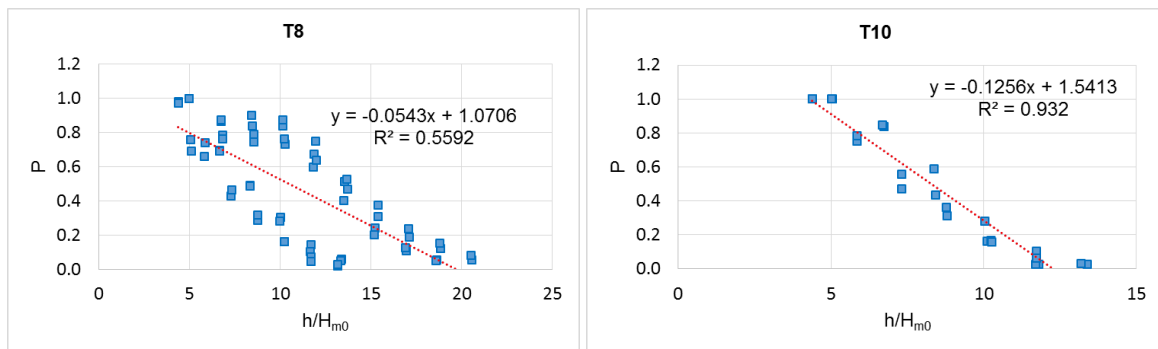


Figure 8. Exceedance probability of splash run-up height on straight face model T8 (no bullnose) and T10 (bullnose)

On the other hand, there are fewer data points which tend to be distributed more closely in cases of those with bullnose. It would be explained that bullnoses effectively prevent splash of low energy but more powerful ones. Therefore, relations between

h_{sp}/H_{m0} and P_{sp} are promisingly expected. For the sake of simplification, linear regressions were performed as deriving function of P_{sp} regarding h_{sp}/H_{m0} as dependent variable, e.g.

$$P_{sp} = -0.095 \frac{h_{sp}}{H_{m0}} + 1.1783 \text{ for curved seawall with bullnose T2} \quad (4)$$

$$P_{sp} = -0.076 \frac{h_{sp}}{H_{m0}} + 1.56 \text{ for steep seawall with bullnose T4} \quad (5)$$

$$P_{sp} = -0.126 \frac{h_{sp}}{H_{m0}} + 1.541 \text{ or straight seawall with bullnose T10} \quad (6)$$

Interestingly, straight seawall without bullnose T8 illustrates the most scattering data while T10 with bullnose offers a regression line of the highest R-squared error. Further works

are encouraged to establish probability distribution function of wave splash run-up height per wave at seawalls with bullnose similar to other representative parameters

including run-up height (Rayleigh) and overtopping volume (Weibull).

CONCLUSION

The paper investigated the wave-seawall interaction regarding overtopping and splashing up through a series of physical model experiments. Different structure models were tested including straight, curved and steep seaward faces which were all shaped with and without bullnose. Measurements reveal the clear effect of bullnose in decreasing wave overtopping. The influence of bullnose becomes less significant with higher waves at curved and straight seawalls; but it is the other way around with steep one. Moreover, bullnoses productively prevent splash of low run-up heights. Simple regression analyses suggest that the exceedance probability of a certain run-up level would be a linear function of the splash run-up levels. The findings may provide more insight into the performance of seawalls with bullnose as well as to properly improve its design in the practice of Vietnam.

Acknowledgements: The research project “A study on producing seawall units with wave-returning bullnose to protect islands, resorts and urban coasts” funded by the Vietnamese Ministry of Construction is acknowledged for providing data.

REFERENCES

- [1] Wang, L., Xie, Y., Wu, Y., Guo, Z., Cai, Y., Xu, Y., and Zhu, X., 2012. Failure mechanism and conservation of the ancient seawall structure along Hangzhou bay, China. *Journal of Coastal Research*, 28(6), 1393–1403. <https://doi.org/10.2112/JCOASTRES-D-12-00036.1>.
- [2] Goda, Y., Kishara, Y., and Kamiyama, Y., 1975. Laboratory investigation on the overtopping rate of seawalls by irregular waves. *Report of the Port and Harbour Research Institute*, 14(4).
- [3] Napp, N., Pearson, J., Bruce, T., and Allsop, W., 2004. Violent overtopping of vertical seawalls under oblique wave conditions. In *Coastal Structures 2003* (pp. 528–541).
- [4] Gotoh, H., Ikari, H., Memita, T., and Sakai, T., 2005. Lagrangian particle method for simulation of wave overtopping on a vertical seawall. *Coastal Engineering Journal*, 47(2–3), 157–181. <https://doi.org/10.1142/S0578563405001239>.
- [5] Pullen, T., Allsop, W., Bruce, T., and Pearson, J., 2009. Field and laboratory measurements of mean overtopping discharges and spatial distributions at vertical seawalls. *Coastal Engineering*, 56(2), 121–140. <https://doi.org/10.1016/j.coastaleng.2008.03.011>.
- [6] Pearson, J., Bruce, T., Allsop, W., Kortenhaus, A., and van der Meer, J. E. N. T. S. J. E., 2005. Effectiveness of recurve walls in reducing wave overtopping on seawalls and breakwaters. In *Coastal Engineering 2004: (In 4 Volumes)* (pp. 4404–4416). <https://doi.org/10.1142/97898127019160355>.
- [7] Hunt, I. A., 1958. Design of seawalls and breakwaters. *US Lake Survey*.
- [8] Besley, P., 1998. Wave overtopping of seawalls, design and assessment manual. *R&D technical report W178*.
- [9] Thomas, R. S., and Hall, B., 2015. Seawall design. *Butterworth-Heinemann*.
- [10] Hughes, S. A., 1993. Physical models and laboratory techniques in coastal engineering (Vol. 7). *World Scientific*.
- [11] Zanuttigh, B., Formentin, S. M., and van der Meer, J. W., 2016. Prediction of extreme and tolerable wave overtopping discharges through an advanced neural network. *Ocean Engineering*, 127, 7–22. <https://doi.org/10.1016/j.oceaneng.2016.09.032>.
- [12] Pullen, T., Allsop, N. W. H., Bruce, T., Kortenhaus, A., Schüttrumpf, H., and van der Meer, J. W., 2007. EurOtop wave overtopping of sea defences and related structures: assessment manual.

- [13] Bruce, T., van der Meer, J., Pullen, T., and Allsop, W., 2010. Wave overtopping at vertical and steep structures. In *Handbook of Coastal and Ocean Engineering* (pp. 411–439). <https://doi.org/10.1142/97898128193070016>.
- [14] Kortenhaus, A., Pearson, J., Bruce, T., Allsop, N. W. H., and van der Meer, J. W., 2004. Influence of parapets and recurves on wave overtopping and wave loading of complex vertical walls. In *Coastal Structures 2003* (pp. 369–381).
- [15] Raichlen, F., Li, Y., Poon, Y., and Boudreau, R., 2001. Splash-Up and Overtopping of Shoreline Structures. In *Coastal Engineering 2000* (pp. 2128–2141). [https://doi.org/10.1061/40549\(276\)166](https://doi.org/10.1061/40549(276)166).